

Impact of the static magnetic field and radiofrequency produced by 7 Tesla

MRI on metallic dental materials

Kenta ORISO¹, Takuya KOBAYASHI^{1*}, Makoto SASAKI², Ikuko UWANO²,

Hidemichi KIHARA¹, Hisatomo KONDO¹

¹Department of Prosthodontics and Oral Implantology, Iwate Medical University

19-1 Uchimaru, Morioka 020-8505, Japan

²Division of Ultrahigh Field MRI, Institute of Biomedical Sciences, Iwate Medical

University

Correspondence to: Hisatomo KONDO, DDS, PhD

Phone: +81-19-651-5111, Fax: +81-19-652-3820, E-mail: hkondo@iwate-med.ac.jp

Short running head: Metallic dental materials at 7 Tesla

Keywords: heating, metallic dental materials, safety, translational attraction, 7 tesla,

ABSTRACT

Purpose: We examined safety issues related to the presence of various metallic dental materials in magnetic resonance (MR) imaging at 7 tesla.

Methods: A 7T MR imaging scanner was used to examine 18 kinds of materials, including 8 metals used in dental restorations, 6 osseointegrated dental implants, 2 abutments for dental implants, and 2 magnetic attachment keepers. We assessed translational attraction forces between the static magnetic field and materials via deflection angles read on a tailor-made instrument and compared with those at 3T.

Heating effects from radiofrequency during image acquisitions using 6 different sequences were examined by measuring associated temperature changes in agarose-gel phantoms with a fiber-optic thermometer.

Results: Deflection angles of the metallic dental materials were significantly larger at 7T than 3T. Among full metal crowns (FMCs), deflection angles were 18.0° for cobalt-chromium (Co-Cr) alloys, 13.5° for nickel-chromium (Ni-Cr) alloys, and 0° for other materials.

Deflection angles of the dental implants and abutments were minimal, ranging from 5.0 to 6.5°, whereas the magnetic attachment keepers were strongly attracted to the field, having deflection angles of 90° or more. Increases in temperature of the FMCs were

significant but less than 1°C in every sequence. The dental implant of 50-mm length showed significant but mild temperature increases (up to 1.5°C) when compared with other dental implants and abutments, particularly on sequences with high specific absorption rate values.

Conclusion: Although most metallic dental materials showed no apparent translational attraction or heating at 7T, substantial attraction forces on the magnetic attachment keepers suggested potential risks to patients and research participants undergoing MR imaging examinations.

INTRODUCTION

Ultrahigh field magnetic resonance (MR) imaging at 7 tesla (T) is one recent advance in medical imaging, and more than 50 such scanners have been installed worldwide. Relative to images acquired by conventional MR imaging at 3T or lower, images acquired at 7T demonstrate remarkably improved spatial and contrast resolution across various imaging sequences, resulting from several substantial advantages at the higher field, including high signal-to-noise ratio (SNR), profound susceptibility effects, large chemical and phase shifts, and prolonged T1 relaxation time [1]. On the other hand, several safety issues augmented at 7T include such unpleasant sensations as vertigo induced by a spatial gradient of the magnetic field [2– 4], interactions of the static magnetic field with metallic materials, and radiofrequency (RF)-induced heating [5,6]. In particular, attractive forces and heating of metallic implants may cause unexpected hazards, so persons with any metallic implant are generally excluded from examinations at 7T.

The safety of metallic implants at 3T or lower has been partially verified, and the results are widely distributed via web pages and review articles [7–12], and safety issues at 7T have recently been assessed for various biomedical implants and devices, such as aneurysmal clips, vascular stents/filters, orthopedic implants, and breast biopsy

markers [5,6]. However, safety concerns regarding the presence of other materials in a 7T scanner remain controversial. Among these, such metallic dental materials as fillings, crowns, and osseointegrated implants, materials that can be present in most potential subjects for MR imaging examinations at 7T, need to be assessed.

We systematically examined interactions of the static magnetic field with various metallic dental materials and RF-related heating effects on these materials during image acquisitions to clarify the safety issues for subjects at 7T.

MATERIALS AND METHODS

Metallic Dental Materials

We examined 18 different metallic dental materials frequently used in clinical practice, including metals for restoration, osseointegrated implants, abutments for implants, and magnetic attachment keepers (Table 1). We cast 8 types of dental metals (Type I gold alloy, Type IV gold alloy, 14K gold alloy, platinum-gold alloy, 12% gold-palladium alloy, silver alloy, cobalt-chromium [Co-Cr] alloy, nickel-chromium [Ni-Cr] alloy) into a full-metal crown (FMC) with the same shape expected in a clinical situation (Fig. 1); examined 6 types of implants (Brånemark System [Bmk; Nobel Biocare, Kloten, Switzerland] Mk III Groovy RP [$\varnothing 4.0 \times 7/10/11.5/13$ mm], Bmk

Zygoma TiUnite [$\phi 4.0 \times 50$ mm], and Spline Twist [$\phi 3.75 \times 11.5$ mm; Zimmer Dental, CA, USA]); 2 types of abutments for implants (Bmk Healing Abutment [$\phi 5 \times 5$ mm], Bmk Temporary Abutment Non-Engaging RP [$\phi 2.5 \times 12$ mm]); and 2 types of magnetic attachment keepers (GIGAUSS D400/D1000; GC, Tokyo, Japan) (Fig. 1).

Assessment of Translational Attraction

We examined interactions between the magnetic field and various metallic dental materials using 7T (Discovery MR950) and, 3T (Discovery MR750, GE Healthcare, Milwaukee, WI, USA) imaging systems. According to the American Society for Testing and Materials (ASTM) F2052-06 [13], we measured the translational attraction of the dental materials by the static magnetic field using the deflection angle test with the device shown in Fig. 2a, as described in a previous report [14]. In this test, each material was suspended by a polyester thread (length 15.0 cm; weight 0.005 mg), and the deflection angle of the thread from the vertical was visually measured using an acrylic plate protractor. These measurements were performed on the axis of the bore ($x = 0$ cm, $y = 0$ cm) (Fig. 2a) and at the position 131 cm (7T) and 85 cm (3T) from the isocenter of the scanner. Our preliminary study (unpublished data) showed the deflection angles of the materials to be largest at these positions.

Assessment of RF-Heating

For the heating test, we measured temperature changes in the metallic materials during image acquisitions using the 7T scanner, according to the previous report [15].

The dental materials were placed parallel to the y-axis of the magnet in a tissueequivalent phantom (14 cm × 10 cm) filled with 1.7% agarose gel and hung by nylon threads along an MR imaging-compatible fiber-optic thermometer probe (Reflex, Neoptix, Québec, Canada) having a temperature resolution of 0.1°C at a depth of 2 cm relative to the surface of the agarose gel (Fig. 2b). A phantom without metallic materials was created as a control. Before measurements were recorded, the phantoms were left in the MR imaging scanner room for one day to achieve equilibrium with the ambient room temperature, which was artificially maintained between 19°C and 20°C with relative humidity (RH) around 50%. We obtained images for each phantom using the 7T scanner, quadrature transmit head coil, and 32-channel head coil with 6 sequences: 2-dimensional (2D) spin-echo (SE) T1-weighted images (T1WIs); 2D-SE T2-weighted images (T2WIs); 3-dimensional (3D) fast SE (FSE) T1WIs; 3D-FSE T2WIs; 3D gradient-echo (GRE) T1WIs using a spoiled gradient recalled acquisition in the steady state (SPGR) technique; and 3D-GRE T2/T1-weighted images (T2/T1WIs) using a fast imaging technique employing steady state acquisition (FIESTA).

Metallic materials within the phantom were placed at the center of the transmit

head coil, where the strength of the electric field is assumed to be maximum. All scans were acquired in first level controlled operating mode. Table 2 shows scanning conditions of the sequences. We measured the temperature of the metallic materials for 6 min at 30-s intervals during image acquisitions, with 10-min intervals between each of the sequences, and then calculated changes in temperature ($\Delta^{\circ}\text{C}$) from the baseline. On the scanner console, we monitored averaged specific absorption rate (SAR) values for the 6 min of acquisition for every combination of the phantoms and sequences. The control and materials that showed the 2 greatest temperature increases were measured 3 times to determine the reproducibility of the measurement.

Statistical Analyses

We used the Wilcoxon signed-rank test to examine differences in the deflection angles of the materials hung in the 7T and 3T scanners; the Wilcoxon signed-rank test with a Bonferroni correction to assess differences in temperature changes between the materials and the control (agarose gel) and those among the materials and to evaluate differences in SAR values and temperature changes among the 6 sequences; and the intraclass correlation coefficient (ICC) to evaluate the reproducibility of the temperature measurements. The alpha level used was 0.05.

RESULTS

We performed the translational attraction test on all the materials. The 2 magnetic attachment keepers were excluded for the heating test because of the extremely strong attraction force of the static magnetic field to these materials.

Assessment of Translational Attraction

Deflection angles of the various metallic dental materials at 7T were significantly larger than those at 3T ($P < 0.01$, Wilcoxon signed-rank test) (Table 1). Among the metals for dental restoration, FMCs of alloys of Co-Cr and of Ni-Cr showed substantial deflection angles of 18.0° (Co-Cr) and 13.5° (Ni-Cr) at 7T compared with those at 3T, 5.5° (Co-Cr) and 4.0° (Ni-Cr). Regarding the other 6 metals, the deflection angle of the FMC was 0° at both 7 and 3T. The deflection angles of the dental implants and abutments were minimal, ranging from 5.0° to 6.5° at 7T and 0.5° to 2.0° at 3T. The magnetic attachment keepers were strongly attracted by the static magnetic field, resulting in a deflection angle of 90° or higher at both 7 and 3T.

Assessment of Heating

Among the 6 imaging sequences at 7T, SAR values were significantly higher in the 2D-SE T1WI (mean, 2.30W/kg), 2D-SE T2WI (2.06W/kg), and 3D-GRE T2/T1WI (2.42W/kg) sequences, compared with the SARs in the 3D-FSE T2WI (1.59W/kg) and

3D-GRE T1WI (1.17W/kg) sequences ($P < 0.01$, Wilcoxon signed-rank test with Bonferroni correction) (Table 2). Increases in temperature during image acquisition were also significantly higher in the 2D-SE T1WI (mean, $0.54 \Delta^{\circ}\text{C}$), 2D-SE T2WI ($0.48 \Delta^{\circ}\text{C}$), and 3D-GRE T2/ T1WI ($0.55 \Delta^{\circ}\text{C}$) sequences when compared with those in the 3D-FSE T2WI ($0.34 \Delta^{\circ}\text{C}$) and 3D-GRE T1WI ($0.29 \Delta^{\circ}\text{C}$) sequences ($P < 0.01$ or < 0.05 , Wilcoxon signed-rank test with Bonferroni correction). The ICC value for the repeated temperature measurements was 0.71, indicating good reproducibility among the measurements. The metals used in dental restorations showed mild temperature changes, from 0.2° to 0.8°C , across the imaging sequences, some of which were significantly higher than those of the control, particularly those on 2D-SE T1WI and 3D-GRE T2/ T1WI ($P < 0.05$, Wilcoxon signed-rank test with Bonferroni correction). The 14K gold alloy and Ni- Cr alloy showed no significant differences in any sequence compared with the control and showed significantly smaller changes compared with the other metals ($P < 0.05$, Wilcoxon signed-rank test with Bonferroni correction) (Table 1). The pure titanium (Ti) dental implants also showed significant increases in temperature compared with the control ($P < 0.05$, Wilcoxon signed-rank test with Bonferroni correction). Among those, the 50-mm long implant (Zygoma TiUnite) showed increases in temperature of 1°C or more on 2D-SE T1WI (1.5°C), 2D-SE T2WI (1.0°C), and

3D-GRE T2/T1WI (1.2°C), which were significantly large when compared with the other dental implants and in any sequences ($P < 0.05$, Wilcoxon signed-rank test with Bonferroni correction) (Table 1, Fig. 3). The dental implant of Ti alloy as well as the abutments for the implants showed minimal, insignificant changes in temperature on any sequence compared with the control (Table 1).

DISCUSSION

Possible risks to subjects and patients of various metallic implants or foreign bodies are one of the issues in clinical research using ultrahigh field MR imaging scanners because attractive forces are proportional to the static magnetic field, and a heating effect is proportional to the square of that [9]. At most institutions, subjects with known metallic implants are not allowed to undergo MR imaging examinations at 7T because little information regarding safety issues at 7T has been provided. Dental materials, such as FMCs and osseointegrated implants, are particularly common in the elderly. Hence, safety assessments of these materials would help expand indications of risk in MR imaging examinations conducted at 7T. In this study, we systematically examined various metallic dental materials, such as metals for restoration, implants, abutments, and magnetic attachment keepers. To our knowledge, this is the first report

regarding safety issues of dental materials at 7T, although those at 3T or below have been reported [15–18].

We examined 8 kinds of metallic materials for dental restoration using FMCs of identical shape cast from the same wax pattern. Among those, 5 kinds of gold alloys and silver alloy demonstrated no attractive forces to the static magnetic field. In contrast, the deflection angles of FMCs made from Co-Cr and Ni-Cr alloys were substantial, 18° (Co-Cr) and 13.5° (Ni-Cr), at 7T and much larger than those at 3T. However, according to the ASTM standard, when the deflection angle is less than 45°, metallic materials are considered safe in terms of translational attraction by static magnetic fields because the force of the magnetic field is less than that of gravity [13]. Moreover, these dental metals are always bonded to the tooth firmly by cement, indicating that there are no risks during MR imaging examination at 7T. These metallic materials showed minimal increases in temperature (0.8°C or less) through image acquisitions, although the temperature rise was significantly larger in some materials than in the control, and the increases were attributed to the eddy current induced in the metals by the time-varying RF field.7 Under scanning within SAR limits, increases in body temperature are usually less than 1.0°C [11]. Hence, an individual with these metals can undergo scans safely even at 7T, although some of the materials demonstrated subtle attraction forces.

Recently, osseointegrated dental implants have been widely applied as prosthetic treatments. Metallic parts for the implants and abutments always consist of pure Ti or Ti alloy and are firmly fixed to the bone or connected together with a the screw. Although most dental implants and abutments are of similar shape, they are available commercially in various lengths. In general, RF-related heating effects depend on the size and length of the metallic materials [19]. In this study, dental implants of 7- to 13-mm lengths, which are frequently used in clinical practice, showed minimal increases in temperature (0.8°C or less) by image acquisitions, whereas the much longer implant of 50-mm length showed significant increases in temperature up (to 1.5°C) when compared with other shorter implants and abutments [19]. Previous studies regarding intraosseous implants revealed that heating more than 47°C can cause injuries to adjacent bone tissues and vessels [20,21]. Hence, dental implants and abutments, including those of substantial length, are considered to hardly cause heating-related injuries of bone and surrounding tissues at 7T. In addition, these materials showed minimal deflection angles of 5.5° or less. It is generally accepted that patients should not feel pain unless implants move in the skeleton. According to the results in this study, the attraction force at such a level should induce no pain even in clinical practice. Osseointegrated dental implants should be considered safe at 7T.

Magnetic attachment keepers are used to stabilize dentures by magnetic forces and firmly cemented to tooth roots or abutments for dental implants. These materials have been reported to show large deflection angles, suggesting probable risks for scanning and severe metallic artifacts on images [16]. In this study, the magnetic attachment keepers were strongly attracted and had deflection angles exceeding 90° at both 7 and 3T, finding comparable to previous results. Thus, individuals with magnetic attachment keepers should be excluded from MR imaging scans at 7T.

In this study, we used 6 kinds of sequences for the heating test because SAR values vary among sequences. In general, the SAR is proportional to the RF duty cycle and to the square of the flip angle. Hence, SE/FSE sequences, particularly T1WI, and the FIESTA sequence show high SAR values. However, these sequences can be optimized to remain within SAR limits provided by the International Electrotechnical Commission (IEC), i.e., 3W/kg (10-min exposure averaged) for MR imaging of the head [22]. In this study, averaged SAR values of these sequences were all less than 2.5W/kg. Even after SAR optimization, the 2D-SE T1WI/ T2WI and 3D-GRE T2/T1WI sequences showed significantly higher SAR values and higher heating effects than the other sequences. Therefore, particularly on the sequences with high SAR, RF-heating of metallic materials should be carefully assessed. In addition, waveform and duration of

the RF pulse should be considered to minimize RF-induced heating, although this issue appears beyond the scope of this study.

Our study has several limitations. First, we did not examine the torque of the metallic dental materials by the static magnetic field. Some materials, such as Co-Cr and Ni-Cr alloys, may show weak torque. However, these materials are always firmly fixed to bone, tooth, or each other, indicating that there are no practical torque-related risks at 7T. Second, mainly because of technical issues, we could not exactly simulate the worst conditions that can affect RF-induced heating, which are described by ASTM F2182 and IEC ISO/TS-10974 [23,24]. Along with size, shape, and composition of materials, heating effects depend on various factors, such as the material's orientation, its position, the relationship between the material and thermometer probe, and the SAR values of each sequence. Subtle but unavoidable inconsistencies of these parameters may affect the results of the heating; for example, the ICC values of repeated measurements were not excellent in this study. Further validation studies fulfilling all the ASTM test methods are needed to reconfirm the safety issues regarding RF-related heating of metallic dental materials. Third, we did not perform the heating test for more than 6min to maintain consistency among sequences and minimize examination time. Scans with longer acquisition time may cause further increases in temperature in these

materials; however, temperature usually rises proportionally with the scanning time,⁵ and even during scans longer than 10 min, it is assumed that temperatures do not even approach hazardous levels. Fourth, we did not examine metallic artifacts induced by the dental materials, which may profoundly deteriorate image quality, because this issue is beyond the scope of this study. Further investigation is needed to clarify this issue at 7 tesla. Finally, this study did not cover other metallic dental materials, such as orthodontic wires and clasps/bars of removable dentures, because these devices can be removed prior to MR imaging examination. These devices consist of Ni-Cr or Co-Cr alloys and can undergo some attractive forces [8], and they may cause RF-heating as well as eddy currents of magnetic field gradients. Removable metallic dental materials remain one of the safety issues at 7T.

CONCLUSION

At 7 tesla, most metallic dental materials, including metals for restoration and osseointegrated implants/abutments, showed no apparent translational attraction or heating, suggesting that these materials can be safe in MR imaging examinations. In contrast, magnetic attachment keepers were strongly attracted by the magnetic field and thus should be prohibited from MR imaging examinations.

ACKNOWLEDGMENTS

We would like to thank T. Metoki for his help in MR imaging examinations.

This work was partly supported by a Grant-in-Aid for Strategic Medical Science Research (S1491001, 2014–2018) from the Ministry of Education, Culture, Sports, Science, and Technology of Japan.

REFERENCES

1. van der Kolk AG, Hendrikse J, Zwanenburg JJ, Visser F, Luijten PR. Clinical applications of 7 T MRI in the brain. *Eur J Radiol* 2013, 82:708-718.
2. Heilmaier C, Theysohn JM, Maderwald S, Kraff O, Ladd ME, Ladd SC. A large-scale study on subjective perception of discomfort during 7 and 1.5 T MRI examinations. *Bioelectromagnetics* 2011; 32:610-619.
3. Theysohn JM, Maderwald S, Kraff O, Moenninghoff C, Ladd ME, Ladd SC. Subjective acceptance of 7 Tesla MRI for human imaging. *MAGMA* 2008; 21:63-72.
4. Uwano I, Metoki T, Sendai F, et al. Assessment of sensations experienced by subjects during MR imaging examination at 7T. *Magn Reson Med Sci* 2014 (epub ahead of print).
5. Dula AN, Virostko J, Shellock FG. Assessment of MRI Issues at 7 T for 28 Implants and Other Objects. *Am J Roentgenol* 2014; 202:401-405.
6. Kangarlu A, Shellock FG. Aneurysm clips: evaluation of magnetic field interactions with an 8.0 T MR system. *J Magn Reson Imaging* 2000; 12:107-111.
7. Shellock FG. Metallic neurosurgical implants: evaluation of magnetic field interactions, heating, and artifacts at 1.5-Tesla. *J Magn Reson Imaging* 2001;

- 14:295-299.
8. Shellock FG. Biomedical implants and devices: assessment of magnetic field interactions with a 3.0-Tesla MR system. *J Magn Reson Imaging* 2002; 16:721-732.
 9. Shellock FG, Crues JV. MR procedures: biologic effects, safety, and patient care. *Radiology* 2004; 232:635-652.
 10. Klockel A, Kemper J, Schulze D, Adam G, Kahl-Nieke1 B. Magnetic field interactions of orthodontic wires during magnetic resonance imaging (MRI) at 1.5 Tesla. *J Orofac Orthop* 2005; 4:279-287.
 11. Schellock FG. Magnetic resonance procedures: health effects and safety. 425-443. CRC Press, New York 2000.
 12. MRI safety.com [<http://www.mrisafety.com>].
 13. American Society for Testing and Materials (ASTM) F2052-06. Standard test method for measurement of magnetically induced displacement force on passive implants in the magnetic resonance environment. West Conshohocken, PA, 2006: F2052-06.
 14. Kuroda K, Shirakawa N, Yoshida Y, Tawara K, Kobayashi A, Nakai T. Evaluation of the magnetic properties of cosmetic contact lenses with a superconducting quantum interference device. *Magn Reson Med Sci* 2014; 13:207-214.

15. Hasegawa M, Miyata K, Abe Y, Ishigami T. Radiofrequency heating of metallic dental devices during 3.0T MRI. *Dentomaxillofac Radiol* 2013; 42:20120234.
16. Miyata K, Hasegawa M, Abe Y, Tabuchi T, Namiki T, Ishigami T. Radiofrequency heating and magnetically induced displacement of dental magnetic attachments during 3.0 T MRI. *Dentomaxillofac Radiol* 2012; 41:668-674.
17. Bra°nemark PI, Hansson BO, Adell R, et al. Osseointegrated implants in the treatment of the edentulous jaw. Experience from a 10-year period. *Scand J Plast Reconstr Surg Suppl* 1977; 16:1-132.
18. Görgülü S1, Ayyildiz S, Kamburoglu K, Gökçe S, Ozen T. Effect of orthodontic brackets and different wires on radiofrequency heating and magnetic field interactions during 3-T MRI. *Dentomaxillofac Radiol* 2014; 43:20130356.
19. Losey AD, Lillaney P, Martin AJ, et al. Safety of retained microcatheters: an evaluation of radiofrequency heating in endovascular microcatheters with nitinol, tungsten, and polyetheretherketone braiding at 1.5 T and 3 T. *J NeuroIntervent Surg* 2014; 6:314-319.
20. Eriksson AR, Albrektsson T, Grane B, McQueen D. Thermal injury to bone. A vital-microscopy description of heat effects. *Int J Oral Surg* 1982; 11: 115-121.
21. Eriksson AR, Albrektsson T. Temperature threshold levels for heat induced bone

tissue injury: a vital-microscopy study in the rabbit. *J Prosthet Dent* 1983; 50:
101-107.

22. International Electrotechnical Commission (IEC). Medical electrical equipment. Particular requirements for the safety of magnetic resonance equipment for medical diagnosis. International Organization for Standardization, Geneva, 2010; 60601-2-33.

23. American Society for Testing and Materials (ASTM) International. Standard test method for measurement of radio frequency induced heating on or near passive implants during magnetic resonance imaging. West Conshohocken, PA, 2011: F2182-11a.

24. International Electrotechnical Commission (IEC). Assessment of the safety of magnetic resonance imaging for patients with an active implantable medical device. International Organization for Standardization, Geneva, 2012; ISO/TS-10974.

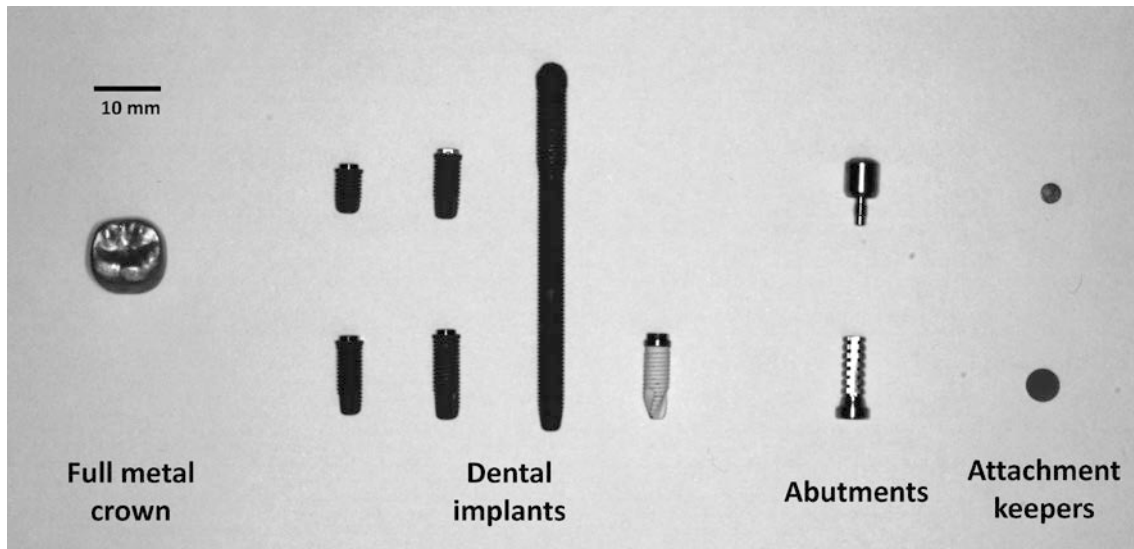


Fig. 1. Metallic dental materials used to examine safety issues at 7 tesla. Left to right; full metal crown ($10.8 \times 8.6 \times 7.8$ mm); osseointegrated dental implants (pure titanium [Ti], $\varphi 4.0 \times 7.0/10.0/10.5/13.0/50.0$ mm; Ti-alloy, $\varphi 3.75 \times 11.5$ mm), abutments of dental implants ($\varphi 5.0 \times 5.0$ mm, $\varphi 2.5 \times 12.0$ mm), magnetic attachment keepers ($\varphi 3.0/4.9 \times 0.6$ mm).

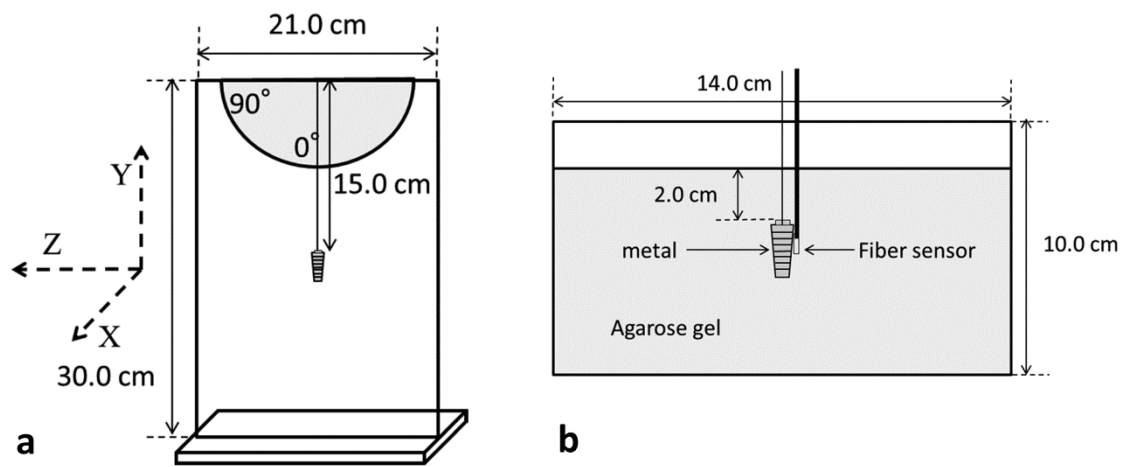


Fig. 2. Measurement devices for deflection angles and temperature changes of metallic dental materials at 7 tesla. (a) Device to measure deflection angles of the materials under static magnetic field. (b) Phantom to measure changes in temperature of the materials during image acquisition.

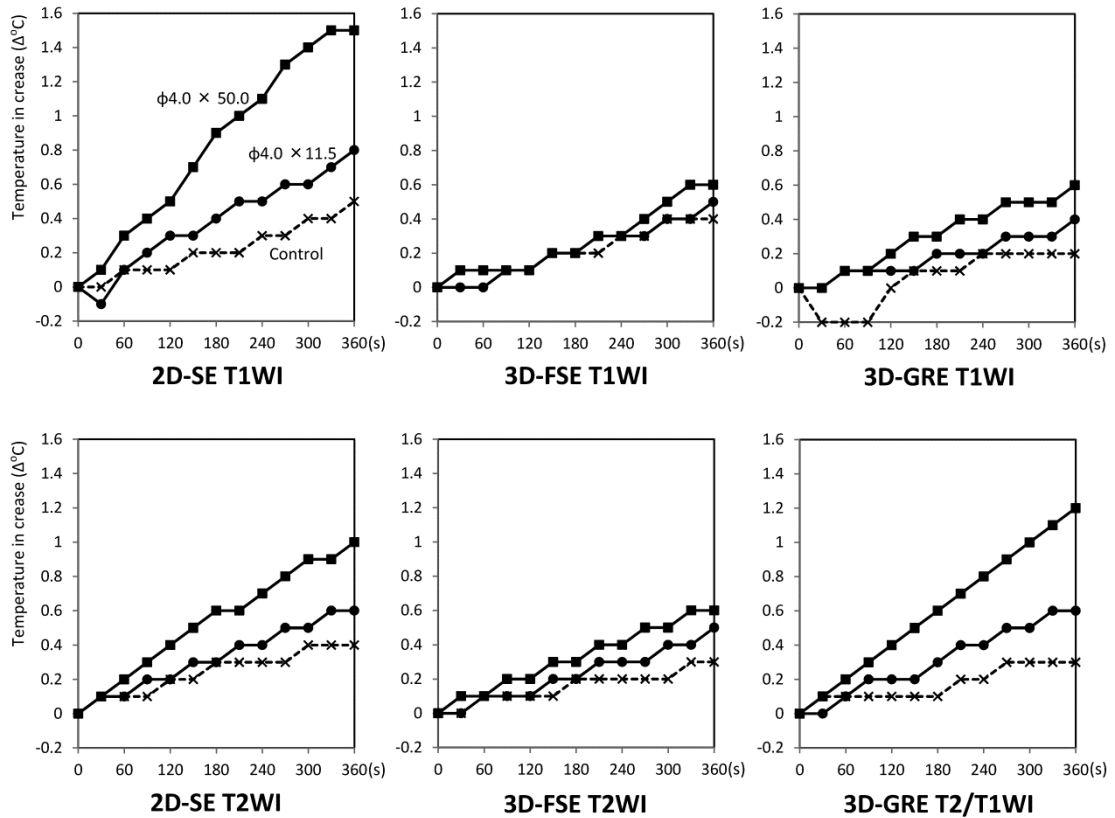


Fig. 3. Temperature changes of dental implants during image acquisitions using various sequences at 7 tesla. Increases in temperature of the pure titanium (Ti) dental implant of $\phi 4.0 \times 50.0$ mm (solid line with squares) are remarkably larger than those of the implant of $\phi 4.0 \times 11.5$ mm (solid line with circles) and the control (agarose gel, dotted line with crosses), particularly on 2D-SE T1WI, 3D-GRE T2/T1WI, and 2D-SE T2WI sequences. 2D, 2-dimensional; 3D, 3-dimensional; FSE, fast spin-echo; GRE, gradient-echo; SE, spin-echo; T1WI, T1- weighted image; T2WI, T2-weighted image; T2/T1WI, T2/T1-weighted image

Table 1. Deflection angle and temperature change of various metallic dental materials

Material type	Trade name	Composition	Specification
Metals for dental restoration	Type I gold alloy	gold (Au) 83%, silver (Ag) 12%, copper (Cu) 5%	Full metal crown (10.8 × 8.6 × 7.8 mm)
	Type IV gold alloy	Au 70%, Cu 16%, Ag 8%, Palladium (Pd) 3%, Platinum (Pt) 2%, others 1%	
	14K gold alloy	Au 58%, Cu 21%, Ag 16%, Pd 3%, zinc(Zn) 2%	
	platinum-gold alloy	Au 83.5%, Pt 10.5%, Ag 1.5%, Pd 1%, others 3.5%	
	12 % gold-palladium alloy	Ag 46%, Pd 20%, Cu 20%, Au 12%	
	Silver alloy	Ag 77%, Tin (Sn) 18%, Zn 5%	
	Co-Cr alloy	cobalt (Co) 63%, chromium (Cr) 29%, molybdenum (Mo) 6%, others 2%	
	Ni-Cr alloy	nickel (Ni) 63%, Cr 15%, niobium (Nb) 5%, manganese (Mn) 5%, others 12%	
Dental implants/ abutments	Bmk Mk III Groovy RP	Titanium (Ti) 99%, others 1%	φ4.0 × 7.0 mm
			φ4.0 × 10.0 mm
			φ4.0 × 11.5 mm
			φ4.0 × 13.0 mm
	Bmk Zygoma TiUnite		φ4.0 × 50.0 mm
	Spline Twist	Ti 90%, aluminum (Al) 6%, vanadium (V) 4%	φ3.75 × 11.5 mm
Magnet attachment keepers	GIGAUSS D400	Fe 72%, Cr 26%, others 2%	φ3.0 × 0.6 mm
	GIGAUSS D1000		φ4.9 × 0.6 mm
Control	–	Agarose gel 1.7%	–

Table 1. (Continued)

Weight (g)	Deflection angle (°)		Change in temperature at 7 Tesla ($\Delta^{\circ}\text{C}$)					
	7 Tesla	3 Tesla	2D-SE T1WI	2D-SE T2WI	3D-FSE T1WI	3D-FSE T2WI	3D-GRE T1WI	3D-GRE T2/T1WI
4.12	0	0	0.4	0.4	0.7*	0.4	0.3	0.7*
3.95	0	0	0.8*	0.8*	0.4	0.5	0.4*	0.6
3.38	0	0	0.3	0.3	0.3	0.3	0.2	0.4
4.65	0	0	0.5	0.8*	0.6*	0.5*	0.4*	0.6
2.55	0	0	0.5*	0.5	0.5	0.5*	0.3	0.7*
2.37	0	0	0.5	0.4	0.4	0.2	0.2	0.5
2.22	18.0	5.5	0.6*	0.3	0.3	0.2	0.2	0.7*
2.22	13.5	4.0	0.3	0.3	0.3	0.3	0.2	0.3
0.22	5.0	1.5	0.3	0.2	0.2	0.2	0.1	0.4
0.30	5.0	2.0	0.6*	0.4	0.4	0.3	0.5*	0.7*
0.33	5.5	0.5	0.8*	0.6	0.5	0.5	0.4*	0.6*
0.42	5.0	1.5	0.4	0.4	0.5	0.3	0.3	0.4
2.38	5.5	1.0	1.5*	1.0*	0.6	0.6*	0.6*	1.2*
0.36	5.0	2.0	0.2	0.4	0.3	0.2	0.1	0.3
0.45	6.5	1.5	0.3	0.4	0.4	0.2	0.2	0.5
0.20	6.0	1.0	0.4	0.3	0.5	0.3	0.2	0.4
0.03	>90	46.0	–	–	–	–	–	–
0.12	>90	>90	–	–	–	–	–	–
–	–	–	0.5	0.4	0.4	0.3	0.2	0.3

Bmk, Brånemark System, Nobel Biocare, Kloten, Switzerland; FSE, fast spin-echo; GIGAUSS D400/D1000, GC, Tokyo, Japan; GRE, gradient-echo; SE, spin-echo; Spline Twist, Zimmer Dental, CA, USA; T1WI, T1-weighted image; T2WI, T2-weighted image; T2/T1WI, T2/T1-weighted image; *P < 0.05 (different from the control, Wilcoxon signedrank test with Bonferroni correction); 2D, 2-dimensional; 3D, 3-dimensional

Table 2. Pulse sequences used for the heating test of metallic dental materials at 7 tesla

	2D-SE T1WI	2D-SE T2WI	3D-FSE T1WI	3D-FSE T2WI	3D-GRE* T1WI	3D-GRE † T2/T1WI
Repetition time (ms)	600	3000	700	3000	10	5.8
Echo time (ms)	9	60	16.5	79	2.7	2.2
Flip angles (°)	90/140	90/140	90/variable	90/variable	15	35
Echo train length	–	–	12	80	–	–
Field of view (mm)	200	200	200	200	200	200
Matrix (freq/phase)	512 × 320	512 × 256	512 × 320	512 × 320	512 × 416	320 × 320
Number of slices	37	37	152	152	152	152
Slice thickness (mm)	3	3	1	1	1	1
Interslice gap (mm)	1	1	0	0	0	0
Band width (kHz)	31.2	31.2	62.5	83.3	62.5	41.7
Number of excitations	3	0.5	1	1	1	1
Acquisition time (min)	6.03	6.12	5.56	6.25	6.39	6.01
SAR (W/Kg) [mean ± SD]	2.30 ± 0.30	2.06 ± 0.25	1.94 ± 0.37	1.59 ± 0.25	1.17 ± 0.12	2.42 ± 0.13

FSE, fast spin-echo; GRE, gradient-echo; SAR, specific absorption rate; SD, standard deviation; SE, spin-echo; T1WI, T1-weighted image; T2WI, T2-weighted image; T2/T1WI, T2/T1-weighted image; 2D, 2-dimensional; 3D, 3-dimensional

*spoiled gradient recalled acquisition in the steady state (SPGR)

†fast imaging employing steady state acquisition (FIESTA)